Journal of Solid State Chemistry **161,** 410–415 (2001)
doi:10.1006/jssc.2001.9356, available online at http://www.idealibrary.com on IDEAL®

Preparation and Characterization of a New Triclinic Compound $Bi_{3.5}V_{1.2}O_{8.25}$ to Show the Known Phase $Bi_4V_2O_{11}$ to Be Nonexistent as a Single Phase

Akiteru Watanabe[1]

Advanced Materials Laboratory, National Institute for Materials Science, 1-1 Namiki, Tsukuba, Ibaraki, 305-0044 Japan

Received May 16, 2001; in revised form July 30, 2001; accepted August 9, 2001

A new compound, $Bi_{3.5}V_{1.2}O_{8.25}$ (25.53 mol% V_2O_5), has been found in the system Bi_2O_3–V_2O_5. It crystallizes in the triclinic symmetry with $a = 16.452(1)$ Å, $b = 16.886(1)$ Å, $c = 7.0914(7)$ Å, $\alpha = 91.330(8)^\circ$, $\beta = 95.186(9)^\circ$, $\gamma = 96.031(9)^\circ$, and $Z = 10$. The structure is considered a superstructure based on a pseudo-fcc subcell with $a' \approx 5.5$ Å, and the transformation matrix is $(\frac{5}{2}, \frac{3}{2}, 0)/(-1,1,3)/(\frac{1}{2},-1,\frac{1}{2})$. This compound yields low conductivity (10^{-4} S cm^{-1} at 500°C); on heating, it decomposes into two unidentified phases at 790°C, and melts at 890°C. Phase equilibrium studies between 25.53 and 50 mol% V_2O_5 have shown that a mixture of $Bi_{3.5}V_{1.2}O_{8.25}$ and $BiVO_4$ is stable at least below 550°C and that the well-known phase $Bi_4V_2O_{11}$ does not exist as a pure phase. Thus, the reported "α-$Bi_4V_2O_{11}$-type" solid solution is a metastable phase. © 2001 Academic Press

Key Words: **new compound $Bi_{3.5}V_{1.2}O_{8.25}$; triclinic symmetry; superstructure; pseudo-fcc subcell; decomposition; metastable; "α-$Bi_4V_2O_{11}$-type" solid solution.**

INTRODUCTION

The compound $Bi_4V_2O_{11}$ (33.33 mol% V_2O_5) was first described by Bush and Venevtsev (1) and was subsequently established as one of the intermediate compounds in the system Bi_2O_3–V_2O_5 (2), where $Bi_4V_2O_{11}$ undergoes two reversible polymorphic transformations at 440°C and at 555°C, and melts incongruently at 880°C. Three modifications are designated as the low-temperature stable α-form, the intermediate β-form, and the high-temperature stable γ-form. On one hand, Abraham *et al.* (3) reported the solid–solubility range (30.7–33.33 mol% V_2O_5) and characterized three modifications of $Bi_4V_2O_{11}$ with the following upper limit composition: the orthorhombic α-form ($a = 16.599$ Å, $b = 5.611$ Å, and $c = 15.288$ Å), the tetragonal β-form ($a = 11.285$ Å and $c = 15.400$ Å at 502°C; correctly, the orthorhombic with $b = a/2$ Å (4)), and the tetragonal γ-form ($a = 4.004$ Å and $c = 15.488$ Å at 702°C). Furthermore, they found a high oxide ion conduction (0.1–1 S cm^{-1}) in γ-$Bi_4V_2O_{11}$. In addition, they succeeded in the γ-$Bi_4V_2O_{11}$ stabilization by the partial substitution of various metal atoms like Cu, Co, etc. (5) for vanadium. At the same time, the stabilized γ-$Bi_4V_2O_{11}$ was named the BIMEVOX series (5), and since then many researchers have paid attention to the series with excellent oxide ion conduction at lower temperatures.

Thus, the BIMEVOX series is based on $Bi_4V_2O_{11}$; however, our experiment showed that a solid-state reaction of the stoichiometric mixture ($2Bi_2O_3 + V_2O_5$) always yielded a two-phase mixture, i.e., mainly the α-form and a small amount of a neighboring compound $BiVO_4$ (50 mol% V_2O_5), as shown in Fig. 1a. Therefore, the pure α-form may have a more Bi-rich composition than $Bi_4V_2O_{11}$. This fact induced us to re-examine subsolidus equilibrium relations in the vicinity of $Bi_4V_2O_{11}$. The results have shown that a new compound $Bi_{3.5}V_{1.2}O_{8.25}$ with triclinic symmetry exists stably and no pure phase is identified at $Bi_4V_2O_{11}$ composition at any subsolidus temperature.

EXPERIMENTAL PROCEDURES

The starting materials were 99.9% pure Bi_2O_3 and V_2O_5. The desired proportions of $Bi_{1-x}V_xO_{1.5+x}$ ($x = 0.2 - 0.35$) were accurately weighed and thoroughly hand-mixed in an agate mortar. The mixture was transferred into a covered platinum crucible and heated at 800–850°C for 20 h or more. At the end of the reaction, the product was quenched by an air stream to room temperature. The same heat treatment was repeated after intermediate grindings to complete the reaction. The product was then put into a gold crucible, annealed at 550°C for 300 h or more, and air-quenched; the reaction was completed by repeating the same annealing process several times. Every time the samples were quenched, they were examined by X-ray powder diffraction (XRPD) using Cu$K\alpha$ radiation and a diffracted-beam monochromator.

[1] Fax: +81-298-52-7449. E-mail: watanabe.akiteru@nims. go.jp.

0022-4596/01 $35.00

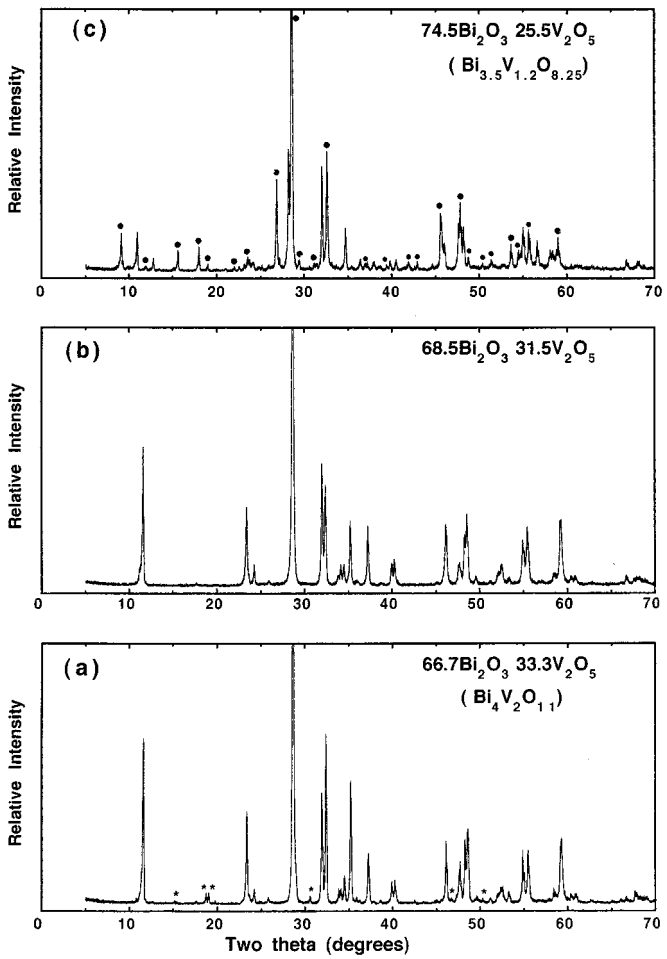

FIG. 1. Room-temperature XRPD patterns of samples equilibrated at 800°C ($\lambda = CuK\alpha$): (a) the composition with 33.33 mol% V_2O_5, (b) 31.50 mol% V_2O_5, and (c) 25.53 mol% V_2O_5. The reflections marked by asteriks in (a) and marked by solid circles in (c) are respectively from $BiVO_4$ and an unidentified phase around 20 mol% V_2O_5.

The composition of the final products was examined by chemical analysis. The bismuth content was determined using a chelatometric titration with EDTA, and the vanadium content was checked using absorbance photometry based on the reaction with hydrogen peroxide.

To check the crystal system and preliminary lattice parameters of a new phase, Visser's indexing program (6) was applied to the observed XRPD data measured with a continuous scanning method at a scanning rate of 0.4° (2θ) min^{-1} over the angular range 5–135° (2θ). The 2θ values were corrected using the external standard of a Si powder.

The density of the powder sample was measured using a gas pycnometer (Micromeritics Accupyc 1330). The sample weight was about 20 g.

The thermal behavior was checked by differential thermal analysis (DTA) with a Rigaku TG-8120 apparatus. About 50 mg of the powder sample in a platinum sample holder underwent heating–cooling cycles in air to the maximum temperature of 915°C. The heating–cooling rates employed were 2, 5, and 10°C min^{-1}. The reference material was α-Al_2O_3, and the temperature accuracy was $\pm$ 3°C.

The *in situ* measurement of phase changes with temperature was carried out in air by high-temperature XRPD using a combination of a MAC Science M21X diffractometer ($CuK\alpha$ radiation) and a MAC Science TXJ-D314 high-temperature device with a platinum sample holder.

Electrical conductivity was measured in air by means of the impedance spectroscopy method on pellets smeared with gold paste as electrodes. To fabricate the pellets, the powder sample was pre-pressed uniaxially (10 mm in diameter and about 2 mm thick), and then pressed isostatically at 200 MPa, and sintered at 750°C for 50 h. The pellets were studied using a Solartron SI-1260 impedance analyzer in the frequency range 1 to 10^6 Hz at every 20°C interval between 150°C and 850°C through a heating–cooling cycle. The sample pellets were equilibrated at constant temperature for 20 to 30 min before each measurement.

RESULTS AND DISCUSSION

Chemical analysis yielded the actual composition of two representative samples as follows: 74.56 $\pm$ 0.03 mol% Bi_2O_3 and 25.44 $\pm$ 0.01 mol% V_2O_5 for $Bi_{3.5}V_{1.2}O_{8.25}$ and 66.69 $\pm$ 0.01 mol% Bi_2O_3 and 33.31 $\pm$ 0.02 mol% V_2O_5 for $Bi_4V_2O_{11}$. Thus, since the compositional changes were negligibly small, the actual compositions are virtually equal to the nominal ones.

Figure 1 shows XRPD patterns of products equilibrated at 800°C with compositions of (a) 33.33, (b) 31.50, and (c) 25.53 mol% V_2O_5. As indicated in Fig. 1a, the composition 33.33 mol% V_2O_5 (i.e., $Bi_4V_2O_{11}$) affords a two-phase mixture consisting of mainly the α-form and a small amount of $BiVO_4$, the reflections of which are marked by asterisks. Although Lee *et al.* (7) reported that pure α-$Bi_4V_2O_{11}$ can be prepared only by rapid cooling from about 850°C, our air-quenched sample with 33.33 mol% V_2O_5 from 850°C gave the same result as Fig. 1a. Joubert *et al.* (8) also reported the same result as Fig. 1a; namely, their XRPD pattern of $Bi_4V_2O_{11}$ prepared at 850°C clearly showed a second phase of $BiVO_4$. Nevertheless, they ignored the presence of $BiVO_4$ on analyzing the structure of α-$Bi_4V_2O_{11}$ by the Rietveld method. In fact, taking into account the $BiVO_4$ content of their sample, the correct composition is not $Bi_4V_2O_{11}$.

According to expectation, the pure α-form is observed at the more bismuth-rich composition, 31.50 mol% V_2O_5 (Fig. 1b) which lies in the middle of the solid–solubility range reported by Abraham *et al.* (30.7–33.33 mol% V_2O_5) (3) and by Lee *et al.* (29.6–33.33 mol% V_2O_5) (7). The product at 25.53 mol% V_2O_5 shown in Fig. 1c is a mixture of two unidentified phases: one has a composition

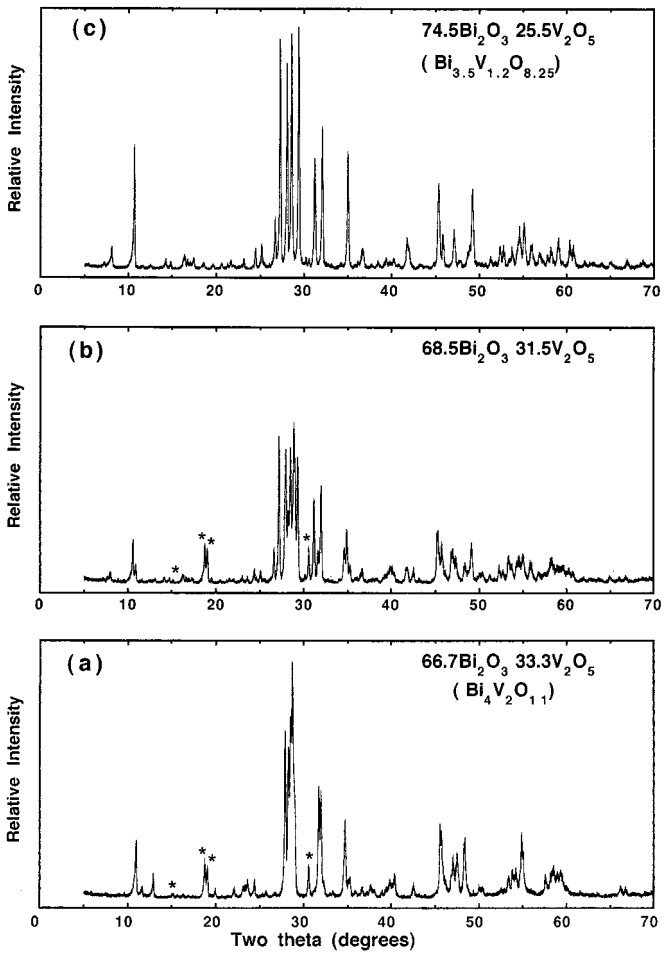

FIG. 2. Room-temperature XRPD patterns of samples annealed at 550°C with the same composition as in Fig. 1 ($\lambda = \mathrm{Cu}K\alpha$). The reflections marked by asterisks in (a) and (b) are from $BiVO_4$.

around 20 mol% V_2O_5 from which reflections are indicated by solid circles in Fig. 1c, and the other is an unknown phase.

Figure 2 shows XRPD patterns of the products annealed subsequently at 550°C. All the patterns change exceedingly, resulting in complicated patterns. It is particularly noteworthy that the α-form disappears almost completely in Fig. 2b. Despite the complexity, the recognizably growing reflections from $BiVO_4$ as asterisked in Figs. 2a and 2b suggest that $BiVO_4$ exists as a constituent phase of a two-phase mixture in the equilibrium state at 550°C. On the other hand, Fig. 2c represents a single phase, i.e., a new compound $Bi_{3.5}V_{1.2}O_{8.25}$ (25.53 mol% V_2O_5). In fact, at every composition not only between 25.53 and 50 mol% V_2O_5 but also less than 25.53 mol% V_2O_5, the product equilibrated at 550°C was a two-phase mixture which was composed of $Bi_{3.5}V_{1.2}O_{8.25}$ and $BiVO_4$ in the former compositional region and $Bi_{3.5}V_{1.2}O_{8.25}$ and the phase marked by solid circles in Fig. 1c in the latter more bismuth-rich range. Although Huvé *et al.* (9) reported that the formation of $BiVO_4$ in only the starting composition of $Bi_4V_2O_{11}$ is due to the introduction of some Bi into the V sites, i.e., $(Bi_2O_2)(V_{1-y}Bi_y)O_z$, we can conclude that the composition of $Bi_4V_2O_{11}$ is situated within a two-phase region on the Bi_2O_3–V_2O_5 phase diagram in the light of the results of Figs. 1 and 2. Therefore, the formation of $BiVO_4$ is inevitable at 33.33 mol% V_2O_5, i.e., $Bi_4V_2O_{11}$.

The thermal stability of the new compound, $Bi_{3.5}V_{1.2}O_{8.25}$, was confirmed by direct preparation through the solid-state reaction of the oxide mixture ($3.5Bi_2O_3 + 1.2V_2O_5$) which was heated from the first at 550°C for a few hundred hours with intermediate grindings; as a result, the same product as in Fig. 3 was obtained. That is, $Bi_{3.5}V_{1.2}O_{8.25}$ can be generated in different ways through the solid-state reaction ($3.5Bi_2O_3 + 1.2V_2O_5$) and through the change of phases produced at 800–850°C as represented in Fig. 1c. Thus, on the basis of the present results, we have reached the conclusion that $Bi_4V_2O_{11}$ never exists as a pure phase, and the reported "α-Bi4V2O11-type" solid solution is a metastable phase which decomposed completely to $Bi_{3.5}V_{1.2}O_{8.25}$ and $BiVO_4$.

The indexing result of the computer program indicated that $Bi_{3.5}V_{1.2}O_{8.25}$ crystallizes in the triclinic system, and the precise lattice parameters were calculated: $a = 16.452(1)$ Å, $b = 16.886(1)$ Å, $c = 7.0914(7)$ Å, $\alpha = 91.330(8)°$, $\beta = 95.186(9)°$, and $\gamma = 96.031(9)°$, and $V = 1950.1(2)$ Å^3. The Miller indices based on these lattice constants are assigned to the reflections as shown in Fig. 3 and as listed in Table 1, which tabulates the observed and calculated d values and relative intensities with $I_{obs} \geq 2$. Inasmuch as the measured density was 7.852(1) g cm^{-3}, it is evident from this value and the cell volume that the triclinic cell contains 10 formula weights, $Z = 10(Bi_{3.5}V_{1.2}O_{8.25})$.

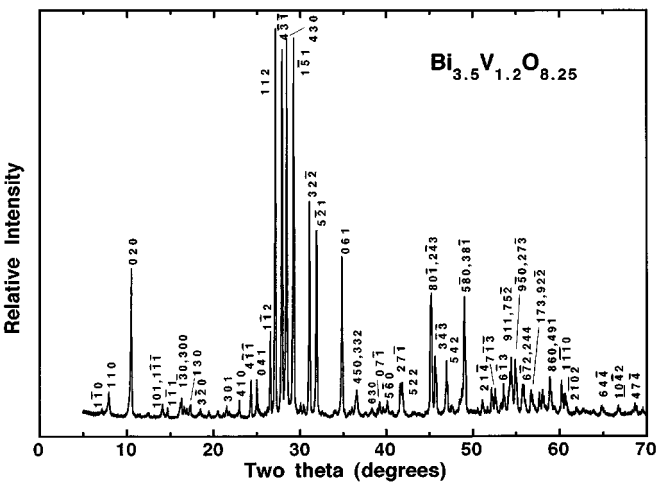

FIG. 3. Room-temperature XRPD pattern of $Bi_{3.5}V_{1.2}O_{8.25}$ equilibrated at 550°C ($\lambda = \mathrm{Cu}K\alpha$).

TABLE 1
X-Ray Powder Diffraction Data for $Bi_{3.5}V_{1.2}O_{8.25}$

h	k	l	d_{calc} (Å)	d_{obs} (Å)	I_{obs}[a]	h'	k'	l'[b]
1	−1	0	12.374	12.384	3			
1	1	0	11.107	11.103	7			
0	2	0	8.392	8.380	38			
0	0	1	7.059	7.053	2			
1	0	1	6.267	6.258	4			
1	−1	−1	6.258					
1	−1	1	6.012	6.008	3			
1	−3	0	5.475	5.476	4			
3	0	0	5.430	5.428	6			
3	−1	0	5.337	5.330	3			
0	2	1	5.316					
2	1	−1	5.237	5.237	3			
1	3	0	5.124	5.117	4			
3	−2	0	4.800	4.794	3			
2	−2	1	4.549	4.552	2			
1	−3	−1	4.324	4.325	2			
2	2	1	4.194	4.191	2			
3	0	1	4.122	4.122	3			
4	0	0	4.072	4.067	2			
3	1	1	3.912	3.914	2			
4	1	0	3.863	3.862	4			
4	−1	−1	3.656	3.654	10			
0	4	1	3.556	3.554	10			
0	0	2	3.529	3.525	3			
0	1	2	3.431	3.430	2			
4	0	1	3.393	3.394	3			
1	−1	2	3.353	3.351	21			
1	1	2	3.283	3.282	100	1	−1	1
4	−3	−1	3.194	3.192	94	1	1	−1
4	3	0	3.136	3.134	95	1	1	1
1	−5	1	3.050	3.049	98	−1	1	1
4	3	−1	2.967	2.967	4			
5	2	0	2.932	2.931	4			
3	2	−2	2.873	2.871	54	0	2	0
5	−2	1	2.799	2.799	49	2	0	0
3	−3	−2	2.745	2.744	2			
6	0	0	2.715	2.714	2			
2	−4	−2	2.637	2.637	2			
3	−3	2	2.6219	2.6217	3			
0	6	1	2.5716	2.5704	42	0	0	2
4	4	1	2.5118	2.5129	2			
5	−4	1	2.4904	2.4903	3			
4	5	0	2.4633	2.4633	4			
3	3	2	2.4520	2.4519	7			
0	5	2	2.3931	2.3939	2			
1	0	−3	2.3601	2.3319	2			
6	3	0	2.3454	2.3453	2			
7	0	0	2.3271	2.3285	2			
3	6	−1	2.3079	2.3078	3			
7	−2	0	2.3073					
0	7	−1	2.2934	2.2933	4			
4	5	1	2.2695	2.2702	3			
5	−6	0	2.2451	2.2450	5			
5	−4	−2	2.2153	2.2146	2			
1	−6	−2	2.1792	2.1794	2			
2	7	−1	2.1669	2.1674	9			
5	2	2	2.1564	2.1559	9			
7	−2	1	2.1410	2.1410	2			
4	5	−2	2.1011	2.1012	2			
3	−1	3	2.0911	2.0904	2			
6	−1	2	2.0710	2.0700	2			
0	8	−1	2.0294	2.0291	2			
8	0	−1	2.0070	2.0069	30	2	2	0
2	−4	3	2.0029	2.0015	30	−2	2	0
3	−4	−3	1.9843	1.9843	16	0	2	−2
5	4	2	1.9326	1.9322	14	2	0	2
8	2	−1	1.9106	1.9101	3			
2	4	3	1.9061	1.9059	3			
4	−8	1	1.8751	1.8752	5			
6	0	−3	1.8664	1.8665	8			
5	−8	0	1.8572	1.8551	30	2	0	−2
3	8	−1	1.8545			0	2	2
9	−1	−1	1.8027	1.8023	3			
5	−8	1	1.7856	1.7854	5			
9	1	−1	1.7656	1.7659	3			
2	1	−4	1.7511	1.7510	8	1	−3	1
7	−1	−3	1.7384	1.7381	7	1	3	−1
7	1	−3	1.7186	1.7185	4			
6	−1	3	1.7082	1.7085	9	3	−1	1
6	7	−1	1.6924	1.6926	7			
9	1	1	1.6876	1.6873	12	3	1	1
7	5	−2	1.6832	1.6830	16	1	3	1
9	−5	0	1.6700	1.6696	14	3	1	−1
2	7	−3	1.6684					
6	−7	2	1.6473	1.6471	9	−3	1	1
2	2	4	1.6417	1.6424	9	2	−2	2
1	7	3	1.6212	1.6213	7	1	−1	3
9	2	−2	1.6170	1.6169	6			
4	9	−1	1.6122	1.6121	3			
8	−6	−2	1.5968	1.5970	6	2	2	−2
4	−9	−2	1.5874	1.5873	7	1	1	−3
8	3	2	1.5779	1.5782	3			
8	6	0	1.5679	1.5663	10	2	2	2
4	9	1	1.5660			1	1	3

[a] Weak reflections (< 2) are omitted to reduce the table.
[b] Miller indices based on the pseudo-fcc subcell.

The XRPD pattern shown in Fig. 3 implies that the triclinic lattice is related to an fcc cell having a lattice constant of about 5.5 Å; in other words, the triclinic structure forms a supercell based on a pseudo-fcc subcell. The fundamental reflections on the subcell are labeled $h'\,k'\,l'$ in Table 1. The comparison of the triclinic indices $h\,k\,l$ with the pseudo-fcc ones $h'\,k'\,l'$ gave the topotactic relationship between the triclinic and pseudo-fcc lattices. The results yielded the transformation matrix for the direct-lattice unit-cell vectors from the pseudo-fcc lattice ($\mathbf{a}', a' \approx 5.5$ Å) to the triclinic one ($\mathbf{a}, \mathbf{b}, \mathbf{c}$): $(\frac{5}{2}, \frac{3}{2}, 0)/(-1, 1, 3)/(\frac{1}{2}, -1, \frac{1}{2})$. Figure 4 exhibits these topotactic relations: $a \approx \sqrt{17/2}a'$, $b \approx \sqrt{11}a'$, and $c \approx \sqrt{3/2}a'$. The value of the determinant of the transformation, 11.75, shows that the volume of the triclinic cell is 11.75 times the size of the pseudo-fcc subcell. Seeing that the fcc cell contains four lattice points, there exist $4 \times 11.75 = 47$ lattice points in the triclinic cell. This result agrees well with the number of cations included in the triclinic cell, i.e.,

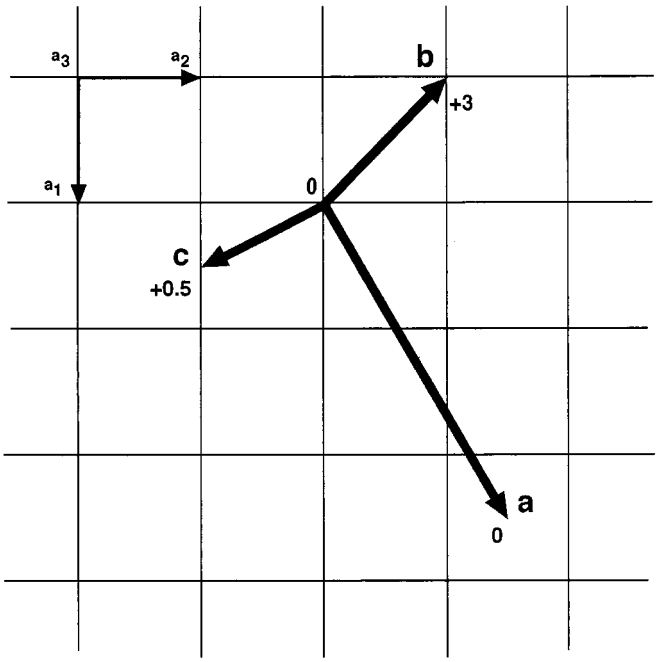

FIG. 4. The unit-cell axis relationships between the triclinic cell (**a**, **b**, **c**) of $Bi_{3.5}V_{1.2}O_{8.25}$ and the pseudo-fcc subcell ($\mathbf{a}_1$, $\mathbf{a}_2$, $\mathbf{a}_3$). The number on each triclinic axis is its coordinate by the subcell unit along the $\mathbf{a}_3$ axis. Cations might occur at pseudocubic corners and face centers.

$Z = 10(Bi_{3.5}V_{1.2}O_{8.25})$. Therefore, the formation of the triclinic phase might be due to the atomic ordering of Bi and V atoms. Likewise, the reported compound $Bi_{23}V_4O_{44.5}$ (14.815 mol% V_2O_5) (10, 11) crystallizes in the triclinic supercell based on a pseudo-fcc subcell similar to the present one. Furthermore, $Bi_{23}V_4O_{44.5}$ shows a high oxide ion conduction up to the congruent melting point of about 950°C without polymorphic transformation, while $Bi_{3.5}V_{1.2}O_{8.25}$ decomposes at about 790°C and exhibits a low electrical conductivity as described below.

Figure 5 represents DTA results of $Bi_{3.5}V_{1.2}O_{8.25}$ with triclinic symmetry: (a) measured at a heating–cooling rate of 10°C min^{-1} and (b) 2°C min^{-1}. The DTA heating curve in Fig. 5a exhibits two endothermic peaks at 851°C and 895°C. The former peak is relatively weak and somewhat broad with an onset temperature of 815°C and the latter peak is traced to the melting. Upon cooling, there are no thermal effects other than one exothermic peak due to the solidifying. The thermal effect at 851°C appears to be irreversible. The slow heating rate of 2°C min^{-1} brings about the diffuseness in the former peak at onset and peak temperatures of 807° and 846°C, respectively, as shown in Fig. 5b. In general, since the slower heating rate makes the sample approach equilibrium more nearly, we employed the data in Fig. 5b; the triclinic phase $Bi_{3.5}V_{1.2}O_{8.25}$ commences to change at 807°C and melts at 893°C.

After DTA measurement, a sample, which was heated to 875°C below the melting temperature and cooled, gave the same XRPD pattern as in Fig. 1c. Likewise, as can be seen from Fig. 6, the high-temperature XRPD yielded the same result: at 800°C the phase change can be observed and at 830°C the change is completed to afford the same pattern as in Fig. 1c. That is, the novel triclinic phase, $Bi_{3.5}V_{1.2}O_{8.25}$, begins to decompose around 800°C to result in two unidentified phases as indicated in Fig. 1c. Once the decomposition has been completed, the triclinic phase is never generated under the usual cooling conditions. In other words, although a rate of decomposition is relatively fast, the reverse reaction to produce the single phase $Bi_{3.5}V_{1.2}O_{8.25}$ proceeds sluggishly.

Figure 7 exhibits the variation of electrical conductivity, $\log(\sigma)$, with temperature for $Bi_{3.5}V_{1.2}O_{8.25}$. The triclinic phase, which shows fairly lower conductivity, commences to decompose obviously at 790°C to bring about two unidenti-

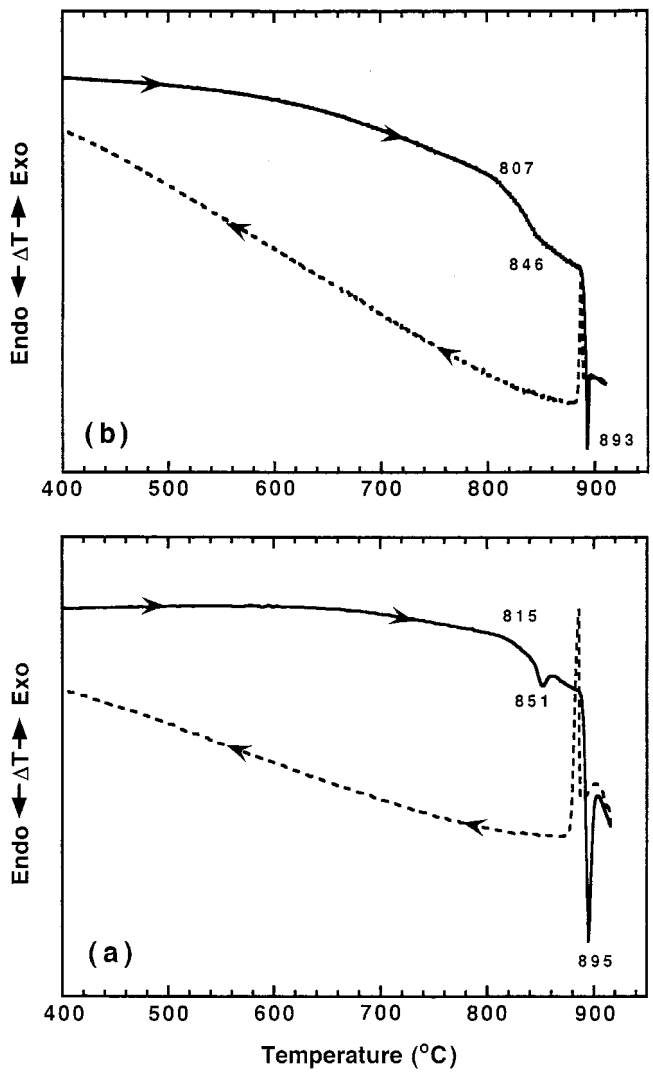

FIG. 5. DTA curves in the heating and cooling cycles for $Bi_{3.5}V_{1.2}O_{8.25}$ at a rate of (a) 10°C min^{-1} and (b) 2°C min^{-1}. The solid lines represent the heating process and the broken lines the cooling process.

fied phases of which the conductivity is higher than for the pristine triclinic phase. Although the DTA results show that the decomposition occurs around 807°C (Fig. 5), both results of the high-temperature XRPD (Fig. 6) and the present $\log(\sigma)$–$1/T$ relationship indicate the decomposition temperature below 800°C. In fact, as mentioned in the Experimental section, the sample prepared at 800°C yields the mixture shown in Fig. 1c; on the other hand, the sample synthesized at 750°C led to the triclinic single phase shown in Fig. 3. Judging from the very broad endothermic peak of the DTA trace (Fig. 5b), the actual decomposition onset temperature must be probably lower than 807°C. Thus, the decomposition temperature was estimated to be 790°C on the basis of the marked $\log(\sigma)$ change in Fig. 7. The phase equilibrium over the range from 20 to 50 mol% V_2O_5 is under investigation.

CONCLUSION

In the system Bi_2O_3–V_2O_5, the new phase $Bi_{3.5}V_{1.2}O_{8.25}$ (25.53 mol% V_2O_5) has been found and characterized. This phase crystallizes in the triclinic symmetry, forms a superstructure based on a pseudo-fcc subcell with $a' \approx 5.5$ Å, decomposes into two unidentified phases at 790°C, and melts at about 890°C. The well-known phase, $Bi_4V_2O_{11}$, which is the base compound of the good oxide ion conductor BIMEVOX series, does not exist as a pure phase. The reported "α-$Bi_4V_2O_{11}$-type" solid solution is a metastable phase which decomposes to a mixture of $Bi_{3.5}V_{1.2}O_{8.25}$ and $BiVO_4$ below 550°C.

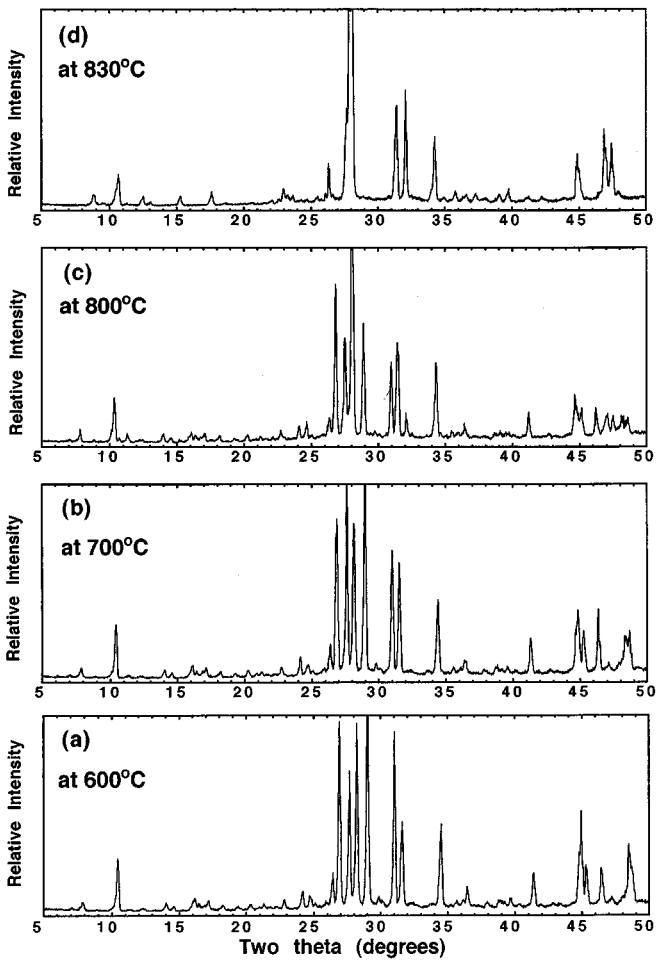

FIG. 6. Series of high-temperature XRPD patterns of $Bi_{3.5}V_{1.2}O_{8.25}$ ($\lambda = CuK\alpha$).

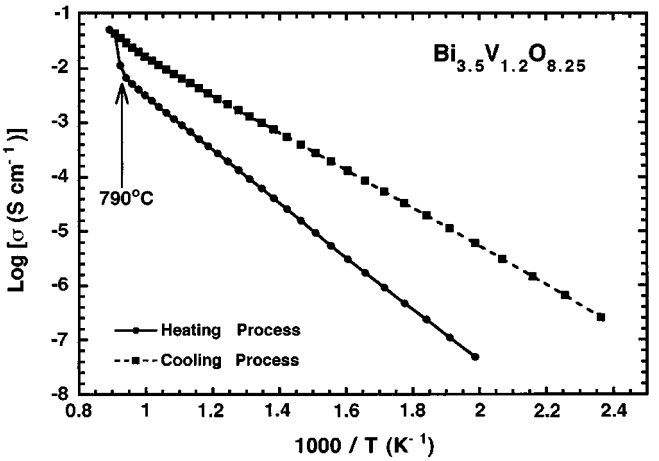

FIG. 7. Arrhenius plots of electrical conductivity σ (S cm^{-1}) of $Bi_{3.5}V_{1.2}O_{8.25}$.

ACKNOWLEDGMENTS

This work was supported by CREST of Japan Science and Technology, and the author thanks Dr. K. Das for the electrical conductivity measurement, Dr. Jiang Dayong for conducting the high-temperature XRPD measurement, and Mr. S. Takenouchi for the chemical analysis.

REFERENCES

1. A. A. Bush and Yu. N. Venevtsev, *Russ. J. Inorg. Chem.* **31,** 769 (1986).
2. Ya. N. Blinovskov and A. A. Fotiev, *Russ. J. Inorg. Chem.* **32,** 145 (1987).
3. F. Abraham, M. F. Debreuille, G. Mairesse, and G. Nowogrocki, *Solid State Ionics* **28–30,** 529 (1988).
4. R. N. Vannier, G. Mairesse, F. Abraham, G. Nowogrocki, E. Pernot, M. Anne, M. Bacmann, P. Strobel, and J. Fouletier, *Solid State Ionics* **78,** 183 (1995).
5. F. Abraham, J. C. Boivin, G. Mairesse, and G. Nowogrocki, *Solid State Ionics* **40/41,** 934 (1990).
6. J. W. Visser, *J. Appl. Crystallogr.* **2,** 89 (1969).
7. C. K. Lee, D. C. Sinclair, and A. R. West, *Solid State Ionics* **62,** 193 (1993).
8. O. Joubert, A. Jouanneaux, and M. Ganne, *Mater. Res. Bull.* **29,** 175 (1994).
9. M. Huvé, R. N. Vannier, G. Nowogrocki, G. Mairesse, and G. V. Tendeloo, *J. Mater. Chem.* **6,** 1339 (1996).
10. A. Watanabe, *Solid State Ionics* **96,** 75 (1997).
11. A. Watanabe, *Solid State Ionics* **113–115,** 601 (1998).